

# INFLUENCE OF DIFFERENT BEAM ENERGIES ON THE MICRO-BUNCHING INSTABILITY

M. Brosi\*, P. Schreiber, M. Schuh, A.-S. Müller,  
Karlsruhe Institute of Technology, Karlsruhe, Germany

## Abstract

During the operation of an electron synchrotron with short electron bunches the beam dynamics are influenced by the occurrence of the micro-bunching instability. This collective instability is caused by the self-interaction of a short electron bunch with its own emitted coherent synchrotron radiation (CSR). Above a certain threshold bunch current dynamic micro-structures start to occur on the longitudinal phase space density. The resulting dynamics depend on various parameters and were previously investigated in relation to amongst others the momentum compaction factor and the acceleration voltage. In this contribution, the influence of the energy of the electrons on the dynamics of the micro-bunching instability is studied based on measurements at the KIT storage ring KARA (Karlsruhe Research Accelerator).

## BEAM DYNAMICS

The micro-bunching instability is not the type of instability which directly leads to total beam loss. More accurately, the micro-bunching instability leads to dynamic changes and deformation of the charge density in the longitudinal phase space, which deteriorates the beam properties. These dynamics are caused by the self-interaction of the bunch with its own emitted CSR. If a bunch is short enough to emit CSR in wavelengths shorter than the waveguide cut-off of the vacuum pipe, the resulting wake-potential acts back on the bunch and causes a change in the energy distribution. The resulting change in the energy distribution is transferred into a change of the longitudinal charge distribution via synchrotron motion. The occurring deformation in the longitudinal bunch profile then causes coherent emission in even higher frequencies which drives the deformation further. In the end, this leads to the formation of dynamic substructures on the charge distribution in the longitudinal phase space rotating with the synchrotron motion.

Depending on the exact parameters, especially the bunch current, this dynamic takes different forms. Below the instability threshold, at low bunch currents, the bunch profile is deformed but stays constant over time (“potential well distortion”). For a certain bunch current, the instability threshold, the bunch profile starts to change periodically as substructures form and rotate in the phase space. At bunch currents significantly above the threshold the dynamic changes again. Now a cycle develops. Substructures start to gain in intensity and grow driven by the wake-potential. Until at one point the filamentation of the substructures in the phase space takes over and they are washed out which leads to an increase of the size in phase space and therefore of the bunch length.

\* miriam.brosi@kit.edu

This significantly reduces the driving wake-potential. The charge distribution now damps down and the bunch length shrinks again until the bunch length is short enough so that the corresponding CSR emission causes a stronger wake-potential again and the cycle starts anew. In the following such a cycle will be referred to as burst, as it corresponds to one outburst in the emitted CSR power which is an easy to measure quantity and indicator for the dynamics.

The characteristics of the micro-bunching instability, like the threshold current or the repetition rate of the bursts depend on multiple beam parameters. Some of which are influenced by the beam energy. So in the following, the influence of the beam energy on the micro-bunching instability is studied based on measurements at a beam energy of 1.3 GeV as well as 0.9 GeV.

## MEASUREMENT

In its role as test-facility KARA provides the flexibility to systematically study the influence of different operation parameters on the micro-bunching instability [1, 2]. Previous studies [3, 4] focused, for example, on the influence of the momentum compaction factor  $\alpha_c$  or the acceleration voltage  $V_{RF}$ , as both parameters influence the bunch length as well as the restoring force in the longitudinal direction. The beam energy also has a big influence on the longitudinal dynamics as it directly changes the radiation damping time and therefore the natural energy spread and the natural bunch length. First measurements of the influence of the longitudinal damping time were conducted by using a CLIC damping ring wiggler prototype [5] to change the synchrotron radiation losses. The results show a change in the repetition rate of the burst while the threshold current and instability frequency directly above the threshold remained unchanged [6].

KARA is a ramping machine with an injection energy of 0.5 GeV and provides besides the standard operation at 2.5 GeV also a short bunch operation mode at 1.3 GeV. To study the influence of the energy an additional short bunch operation mode was established at 0.9 GeV. The transverse tunes were chosen close to the ones of the 1.3 GeV short bunch mode. Optics at several different values of  $\alpha_c$  were implemented.

To observe the dynamics of the micro-bunching instability, the emitted CSR was measured with a quasi-optical broadband Schottky barrier diode detector [7]. The detector signal was read out with KAPTURE a fast data acquisition system which allows a continuous turn-by-turn and bunch-by-bunch read-out [8].

As the dynamic of the instability strongly depends on the bunch current and KARA, as ramping machine, does not provide top-up operation, the emitted CSR power was measured for each setting over a bunch current decay. The fluctuation frequencies of the measured CSR power give direct insight into the time scales of the dynamics of the instability. These fluctuation frequencies are typically displayed in form of a spectrogram as a function of the bunch current as shown in Fig. 1.

## RESULTS

The measurements in Fig. 1a and Fig. 1b were taken at similar values of  $\alpha_c$  and  $V_{RF}$  which results due to the difference in energy in a different bunch length. Contrary to that, the measurements in Fig. 1a and Fig. 1c were taken at a similar natural bunch length (which was achieved by operating at different values of  $\alpha_c$  and  $V_{RF}$  for the different energies).

In all three spectrograms the same characteristic structures can be seen but their positions and exact shapes differ. A finger-like structure is visible which decreases in frequency with decreasing bunch current and ends in a narrow frequency line at the instability threshold (often referred to as initial instability mode/frequency). The threshold current below which nearly no fluctuations are observed<sup>1</sup> differ quite drastically between the measurement at 1.3 GeV ( $\approx 0.159$  mA) and the measurements at 0.9 GeV ( $\approx 0.040$  mA and  $\approx 0.055$  mA).

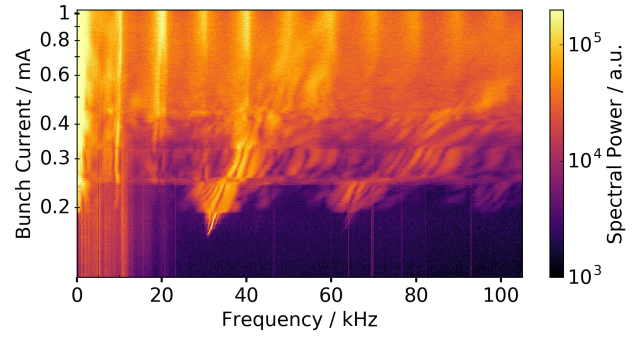
Nevertheless, the measured thresholds fit quite well to the prediction in [9]. This can be seen in Fig. 2. The representation in the dimensionless parameters<sup>2</sup>  $\Pi$  and  $S_{CSR}$  show that they coincide with the predicted linear dependence of the threshold  $(S_{CSR})_{th} = 0.5 + 0.12 \Pi$ . Even the additional area of instability due to the weak instability occurring for settings with even shorter natural bunch length coincides for 0.9 GeV and 1.3 GeV.

The repetition rate of the burst is only visible as bright area at the left edge of the spectrograms in Fig. 1 as the frequency is much lower than the rest of the dynamics. It is therefore in the following referred to as low bursting frequency. Figure 3 shows the low bursting frequency extracted as a function of bunch current for several measurements at different values of  $\Pi$  for 1.3 GeV (Fig. 3a) and 0.9 GeV (Fig. 3b). For both energies a similar behavior is visible. The low bursting frequency is roughly constant at higher bunch currents but varies for lower bunch currents. Noteworthy is that the absolute values of the frequency are systematically lower in the 0.9 GeV measurements, for the typical value at higher bunch currents ( $\sim 90$  Hz vs.  $\sim 270$  Hz) as well as for the span at lower currents ( $\sim 60$  Hz to  $\sim 300$  Hz) vs. ( $\sim 180$  Hz to  $\sim 900$  Hz)).

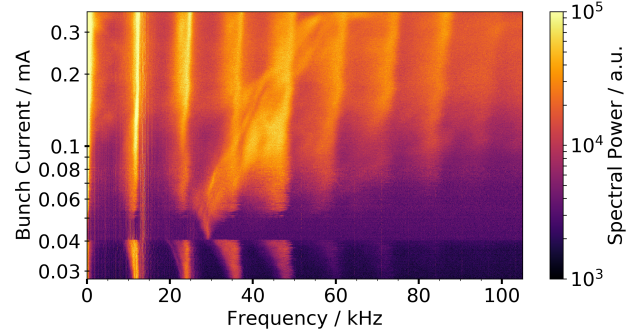
There is an approximate factor of 3 between the frequencies at 0.9 GeV and 1.3 GeV. This coincides with the in-

<sup>1</sup> With an exception for the measurement in Fig. 1b where directly below the threshold at  $\approx 0.04$  mA another instability (the weak instability [4,9]) starts.

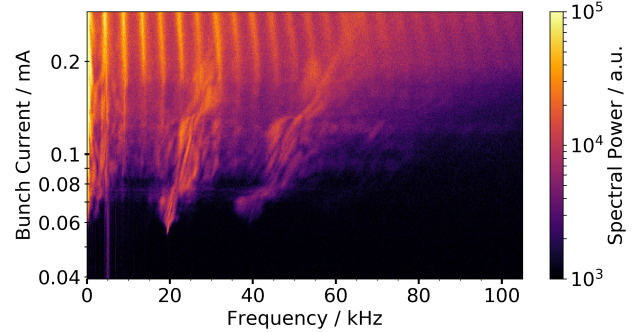
<sup>2</sup>  $\Pi = \frac{\sigma_{z,0} \rho^{1/2}}{h^{3/2}}$ ,  $S_{CSR} = \frac{I_n \rho^{1/3}}{\sigma_{z,0}^{4/3}}$  with  $I_n = \frac{\sigma_{z,0} I_b}{\alpha_c \gamma \sigma_\delta^2 I_A}$ , see [4]



(a) 1.3 GeV,  $\alpha = 4.8 \cdot 10^{-4}$ ,  $V_{RF} = 1500$  kV  
 $\rightarrow \sigma_{z,0} = 3.3$  ps



(b) 0.9 GeV,  $\alpha = 5.1 \cdot 10^{-4}$ ,  $V_{RF} = 1500$  kV  
 $\rightarrow \sigma_{z,0} = 1.9$  ps



(c) 0.9 GeV,  $\alpha = 3.6 \cdot 10^{-4}$ ,  $V_{RF} = 300$  kV  
 $\rightarrow \sigma_{z,0} = 3.6$  ps

Figure 1: Spectrograms showing the fluctuation frequencies in the measured CSR power in the THz frequency range as a function of bunch current. (a) and (b) show measurements at similar settings of  $\alpha_c$  and  $V_{RF}$  but different beam energies (1.3 GeV and 0.9 GeV) resulting in a different natural bunch length  $\sigma_{z,0}$ . The measurement in (c) was also taken at 0.9 GeV but with a natural bunch length similar to the measurements in (a).

verse change in radiation damping time  $\tau$  from 31.7 ms (at 0.9 GeV) to 10.4 ms (at 1.3 GeV). So, for 0.9 GeV where the radiation damping is slower the repetition rate of the burst is lower. The direction of this change fits well to the dynamics during one burst as described in the beginning. The observed factor of  $1/\tau$  is only a rough approximation over the total of all measurements shown in Fig. 3. When comparing single measurements with similar settings at different energies this factor would probably vary. Especially, since depending on the analysis objective, similarity could mean different combinations of settings and therefore yield different results.

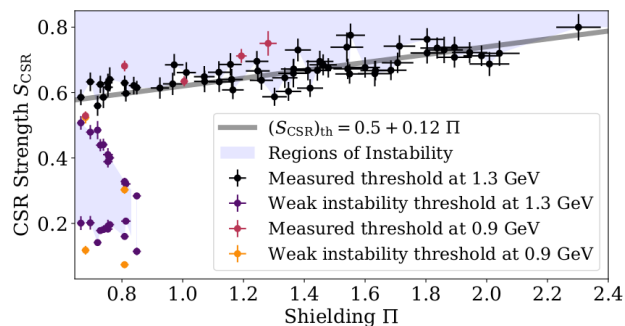


Figure 2: The measured instability thresholds as well as the prediction by [9] are shown using the dimensionless shielding parameter  $\Pi$  and  $S_{CSR}$ . The measured thresholds for both beam energies agree with the prediction and show both the additional region of instability (weak instability) [4, 9] at lower values of  $\Pi$  ( $\approx$  shorter natural bunch length).

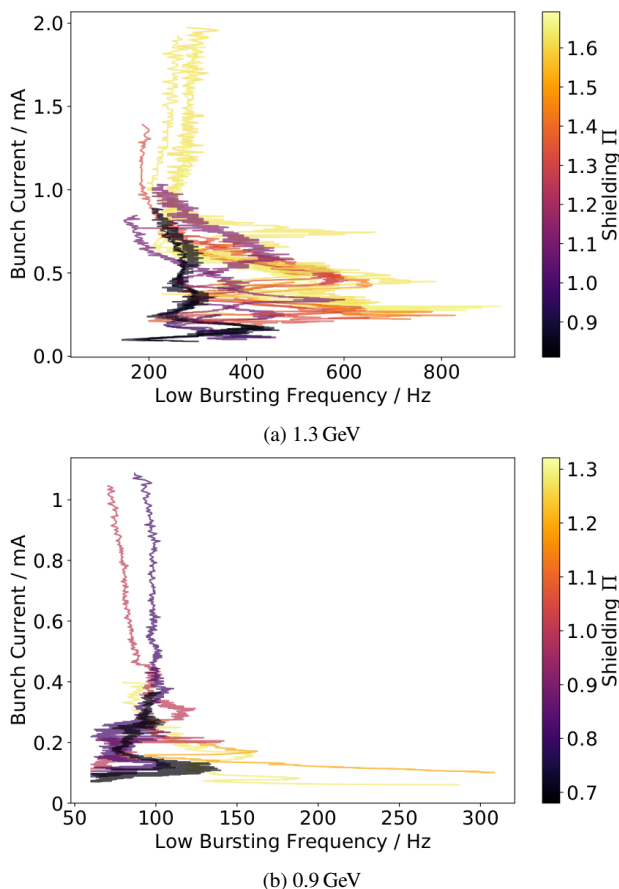


Figure 3: The low bursting frequency corresponds to the repetition rate of the outburst during the micro-bunching instability. It is shown for measurements at different values of  $\Pi$  as a function of the bunch current. (a) For a beam energy of 1.3 GeV the frequency spans approx. from 180 GHz to 900 GHz. (b) While for 0.9 GeV the frequency spans approx. from 60 GHz to 300 GHz. For both energies the measurements show a wider span for higher values of  $\Pi$  which corresponds to settings with a longer natural bunch length.

Also, it needs to be checked if the observed factor of  $1/\tau$  is consistent over different energies by conducting additional measurements at further values of the beam energy.

In [6, 10] a simplified model for the temporal development of the bunch length during a burst was established. It assumes that the duration of a burst consists of two parts. In the first ( $\Delta t_{rise}$ ) the bunch length increases due to the substructures increasing and filamenting out. And in the second ( $\Delta t_{shrink}$ ) the bunch length is damped down as the driving wake potential is small due to the now smoother distribution. For a small enough wake potential, this can be assumed as an exponential decay with the longitudinal damping time from the maximal blown-up bunch length  $\sigma_{z,max}$  down towards the natural bunch length  $\sigma_{z,0}$ . The decay stops at a minimal bunch length  $\sigma_{z,min}$  as soon as the wake potential becomes non-negligible due to the now shorter bunch length and drives the formation of new substructures. The  $1/\tau$  dependency observed in the measurements is not directly obvious from that model. While the damping time is a linear factor in  $\Delta t_{shrink}$  the beam energy also changed  $\sigma_{z,0}$  and probably  $\sigma_{z,min/max}$  as well as  $\Delta t_{rise}$ .

Therefore, the next steps will be to further investigate the influence of the energy, e.g. by measurements at additional energies and employing a VFP solver. Adjusting the simple model described above and figuring out the energy dependence of the different terms to fit the simple model to the measurements could provide an insight into the driving parts behind the dynamics. It could, for example, strengthen the understanding of why at one point the substructures are not driven further but start to filament out so that the charge distribution in phase space is damped down to a small enough bunch length to start a new burst again.

## CONCLUSION

The micro-bunching instability is a longitudinal, coherent instability caused by the self-interaction of a bunch with its own emitted coherent synchrotron radiation. A complex dynamic unfolds in the charge distribution in the longitudinal phase space with the formation of dynamic substructures leading to changes in the bunch profile and length. In comparison of measurements taken at 0.9 GeV and 1.3 GeV significant changes in the dynamics could be observed due to the difference in beam energy. The observed decrease in the threshold current fits well to the predictions. Additionally a change of the low bursting frequency (the repetition rate of the burst during the instability) by an approximate factor of  $1/\tau$  was observed.

## REFERENCES

- [1] A.-S. Müller *et al.*, “Far Infrared Coherent Synchrotron Edge Radiation at ANKA”, in *Proc. 21st Particle Accelerator Conf. (PAC’05)*, Knoxville, TN, USA, May 2005, paper RPAE038, pp. 2518-2520.
- [2] M. Klein *et al.*, “Modeling the Low-Alpha-Mode at ANKA with the Accelerator Toolbox”, in *Proc. 24th Particle Accelerator Conf. (IPAC2012)*, New York, USA, June 2012, paper THP038, pp. 2518-2520.

- ator Conf. (PAC'11)*, New York, NY, USA, Mar.-Apr. 2011, paper WEP005, pp. 1510–1512.
- [3] M. Brosi *et al.*, “Fast mapping of terahertz bursting thresholds and characteristics at synchrotron light sources”, *Phys. Rev. Accel. Beams*, vol. 19, p. 110701, Nov. 2016.  
doi:10.1103/PhysRevAccelBeams.19.110701
- [4] M. Brosi *et al.*, “Systematic studies of the microbunching instability at very low bunch charges”, *Phys. Rev. Accel. Beams*, vol. 22, p. 020701, Feb. 2019.  
doi:10.1103/PhysRevAccelBeams.22.020701
- [5] A. Bernhard *et al.*, “A CLIC Damping Wiggler Prototype at ANKA: Commissioning and Preparations for a Beam Dynamics Experimental Program”, in *Proc. 7th Int. Particle Accelerator Conf. (IPAC'16)*, Busan, Korea, May 2016, pp. 2412–2415. doi:10.18429/JACoW-IPAC2016-WEPMW002
- [6] M. Brosi *et al.*, “Studies of the Micro-Bunching Instability in the Presence of a Damping Wiggler”, in *Proc. 9th Int. Particle Accelerator Conf. (IPAC'18)*, Vancouver, Canada, Apr.-May 2018, pp. 3273–3276.  
doi:10.18429/JACoW-IPAC2018-THPAK029
- [7] ACST GmbH, <http://www.acst.de/>.
- [8] M. Caselle *et al.*, “An ultra-fast data acquisition system for coherent synchrotron radiation with terahertz detectors”, *J. Instrum.*, vol. 9, p. C01024, Jan. 2014.  
doi:10.1088/1748-0221/9/01/C01024
- [9] K. L. F. Bane, Y. Cai, and G. Stupakov, “Threshold studies of the microwave instability in electron storage rings”, *Phys. Rev. ST Accel. Beams*, vol. 13, p. 104402, Oct. 2010.  
doi:10.1103/PhysRevSTAB.13.104402
- [10] M. Brosi, “In-Depth Analysis of the Micro-Bunching Characteristics in Single and Multi-Bunch Operation at KARA”, Ph.D. thesis, Phys. Dept., Karlsruher Institut für Technologie, Karlsruhe, Germany, 2020.  
doi:10.5445/IR/1000120018.